*Sensors & Transducers, Vol. 175, Issue 7, July 2014, pp. 234-243*

**Sensors & Transducers**



# A Research on Damage Mechanics of Dynamic Reliability

**[1, 2] Xiaogang Qu, [2] Gening Xu, [2] Xiaoning Fan**

[1] College of Mechanical Electronic Engineering, Lanzhou University of Technology, Lanzhou 730050, China

[2] College of Mechanical Engineering, Taiyuan University of Science and Technology, Taiyuan 030024, China

[1] Tel: +8613403692910

[1] E-mail: titanic198036@126.com, 23162215@qq.com

*Received: 1 July 2014 /Accepted: 28 July 2014 /Published: 31 July 2014*

**Abstract:** By taking the axial tension member as an example, the damage caused by the cyclic stress influencing reliability was researched. According to the damage mechanics theory, some micro-cracks were observed in the material with cyclic load. With the increase of times loads inflicting, the fresh micro-cracks were formed; meanwhile, the existing cracks further extended, consequently, the effective bearing area reduced and the effective stress increased. By using the model of stress-strength interference, ignoring the effects of erosion and aging on the strength degradation, effective stress increasing lead by the change of damage were only taken into account. This research took the intensity as a random variable and view stress as a random variable which changed with the times of loading, and combined physical experiments and simulation of sampling. Furthermore, the dynamic reliability curve of the stress of tension member that changes with the loading times was simulated; the changing trends of dynamic reliability under different cyclic loading at the same temperature and the same cyclic loading at different temperatures were analyzed respectively. The results suggested that the reliability presents a downward trend when the life is about 80 %, the dynamic reliability curve shows a typical bathtub curve in the later two steps. *Copyright © 2014 IFSA Publishing, S. L.*

**Keywords:** Damage mechanics, Fatigue damage, Damage evolution model, Stress strength interference, Dynamic reliability.

## 1. Introduction

The traditional reliability model is calculated directly by the stress strength interference theory with known stress and distribution of strength. However, the reliability calculated was considered to be the static reliability [1, 2]. The research of dynamic reliability is more complicated than that of static reliability. Salvatore [3] and Chaudhuri [4] have studied the dynamic reliability. However, their research did not analyze the influence of time on strength and stress. Prof. Xie Liyang in Dongbei University and Zuo Yongzhi in Tsinghua University have much attentions on dynamic reliability [5-8], however, the law of strength degradation was difficult to be obtained in the engineering applications. This paper proposed a dynamic reliability calculation method based on damage mechanics using traditional reliability calculation method and the damage mechanics theory. This calculation method is of explicitly physical significance.

In the practical engineering, mechanical components and parts are influenced by many factors

such as the environments, stress and strength. With the stretch of time consumed, the strength is tending to be degraded. So reliability quota is a dynamic and digressive process with the increase of time. The degradation of strength can be divided into two parts: the factors relating to time, such as erosion and aging, and the fatigue damage caused by cyclic load relates to many factors, such as loading times, loading sizes and loading frequency, etc.

SSI (Stress Strength Interference) has been widely applied in practical engineering. The interference area that random variable stress and random variable strength distribute is the ineffective area; while, strength is considered as a time random process in practical engineering. With the increase of frequency and time of loading, the strength tends to be degraded. Fig. 1 shows that with the stretch of time, intersecting area increases step by step. This finally leads to the decrease of reliability.

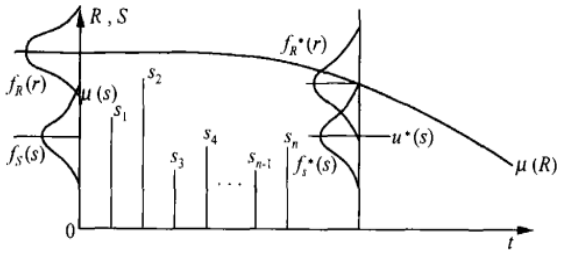


**Fig. 1.** Strength degradation trends change with time.

Degradation of strength is resulted from the defects and cracks in the material. This is due to that material in the cyclic alternating stress results in decrease of mechanical property.

Damage value is indicated as $D$ using damage mechanical method. After being damaged, effective stress is obtained by using $D$ . The increasing process of effective stress is as same as that of strength degradation. Such process increases with the stretch of loading times. Assuming strength degradation is caused by fatigue damage lead by loading. The strength influenced by erosion and aging is not taken into account. It is as considered as the increasing process of stress. As shown in Fig. 2, with the stretch of time, stress and intersecting area increase gradually. This leads to decrease of reliability quota decrease.

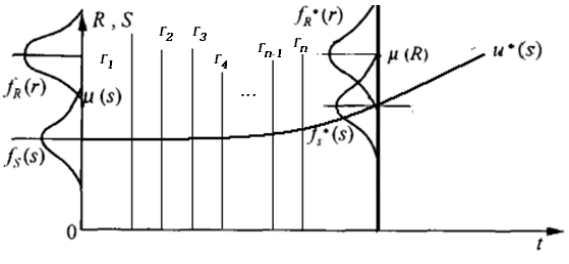


**Fig. 2.** Stress increases trends change with time diagram.

Existing calculation methods fail to describe the influence of loading times on structure reliability on the view of material damage. However, the influencing role of load loading times on the material mechanical properties can describe the theory in detail. The effective stress increase indirectly reflects the strength degradation, the theory can be applied into the stress strength interference theory and well solve the problems in the dynamic reliability analysis.

## 2. Fatigue Damage Theory

According to damage mechanical theory [9], damage variable $D$ stands for the expansion of micro-void. And Micro cracks lead the material into the damage real effective bearing area $\tilde{A}$ which is denotes as decrease degree. That's to say, formation and extending of micro-cracks and micro-gaps result in cross-sectional area $A$ of test specimens reduce to practical effective loaded area $\tilde{A}$; Meanwhile, the diminution of effective loaded area results in the increase of practical stress, which leads to degradation of mechanical property of materials. According to the definition of damage mechanics assume:

$$1-D=\tilde{A}/A \tag{1}$$

The cross section effective bearing area reduced, lead to the increase of effective stress, effective stress can be expressed as:

$$\tilde{\sigma}=\sigma/(1-D) \tag{2}$$

### 2.1. Fatigue Damage Model

The fatigue damage is caused by the material with lower ultimate strength under the alternating load. Some local area or wide area first yield, plastic deformation of high degree is found in a local region, it is a kind of the fracture process of its trans-granular fracture.

Based on continual damage mechanics theory, fatigue damage is expressed by dissipation potential function. This text use X. H. Yang, N. Li, *et al*., proposed dissipation potential model [10], to express the degree of damage accumulation:

$$\phi=\frac{Y^2}{2S_0}\frac{\dot{r}}{(1-D)^{a_0}}, \tag{3}$$

where:

$S_o$ is the materials relates to the temperature constant;

$a_o$ is the material constant;

$\dot{r}$ is the each cycle of accumulated plastic strain.

According to the literature [11], the extent of damage accumulation is described by function $\beta(\sigma,T)$ instead of $a_o$; experimental cyclic load is pulsation cycle, $\sigma$ is expressed by the biggest stress '$\sigma_{\max}$', Expression (4) is

$$\phi = \frac{Y^2}{2S_0}\frac{\dot{r}}{(1-D)^{1-k(\sigma_{\max},T)}} \tag{4}$$

Literature [12] explained the theory of fatigue damage in detail. Assuming that plasticity deformation leads to interior damage and energy consumption, so dissipation potential function is

$$\phi = \phi_P(\sigma,\sigma_Y,R,D) + \phi_D(Y,r,T,\varepsilon_e,D), \tag{5}$$

where:

$\sigma$ is the stress tensor;

$\sigma_Y$ is the Material the initial yield stress;

$R$ is the Isotropic cumulative plastic strain hardening parameters;

$Y$ is the strain energy release rate;

$r$ is the accumulated plastic strain;

$T$ is the absolute temperature;

$\varepsilon_e$ is the elastic strain tensor;

$\phi_P$ is the elastic strain tensor, in view of the loss of plastic parts;

$\phi_D$ is the dissipation part of the damage.

In view of the damage dissipation part $\phi_D$, damage kinetics law can be expressed as:

$$\dot{D} = -\frac{\partial\phi_D}{\partial Y}\dot{\lambda} = -\frac{\partial\phi}{\partial Y} \tag{6}$$

Substituting Equation (4) into (6), we obtain

$$\dot{D} = (-\frac{Y}{S_0})\frac{\Delta\dot{r}}{(1-D)^{1-k(\sigma_{\max},T)}} \tag{7}$$

The strain energy release rate is

$$Y = -\frac{\sigma_{eq}^2}{2E(1-D)^2}R_V \tag{8}$$

Here

$$\Delta\tilde{\sigma}_{eq} = \frac{\sigma_{eq}}{1-D}$$

Based on strain equivalence principle , the stress-strain relations is

$$\Delta\tilde{\sigma}_{eq} = K\Delta r^{\mathrm{m}}, \tag{9}$$

where *K*, *m* are the constants.

Substituting (8) and (9) into (7), Equation (10) can be obtained:

$$\dot{D} = (-\frac{K^2R_V}{2ES_0})\frac{\Delta r^{2m}}{\left[(1-D)\right]^{1-k(\sigma_{\max},T)}}\Delta\dot{r} \tag{10}$$

Integrating Equation (10), and $D = N/N_f$, the boundary conditions $D\big|_{N=N_0} = D_0, D\big|_{N=N_f} = 1$ are generated,

$$D = 1-(1-D_0)[(1-N/N_f)]^{k(\sigma_{\max},T)} \tag{11}$$

Equation (11) is deduced based on damage mechanics theory of fatigue damage evolution model.

### 2.2. Damage Variable Selection

By selecting the axial deformation under tensile state changes in the average strain as a damage variable,

$$D = \varepsilon_N / \varepsilon_f \tag{12}$$

where $\varepsilon_N$ is the average strain in the process of circulation; $\varepsilon_f$ is the average strain when the material is fracture.

## 3. Stress Strength Interference Theory

The stress bored by product exceeds the strength of material, so the product loses effectiveness. Stress exceeds yield stress; meanwhile, material yield occurs, stress exceeds the limitation of strength, crack appears. The strength of product is different with different material characters, structures and producing process. The size of strength can be expressed by a random variable, the size of stress that product bears is a random variable. In the random time of normal working process, the strength is always bigger than the stress, once the stress exceeds the strength, the product will lose effectiveness. This is SSI. Strength stands for the biggest stress ability that the product bears. According to ineffective process, reliable analysis can be preceded by analyzing interaction between product stress and strength.

The stress strength interference model is

$$M = R - S \tag{13}$$

where *R* is the intensity of specimen; *S* is the stress on the specimen; *R, S* are the contains the function of many variables

$$R = R(\mathrm{X}) = \mathrm{R}(\mathrm{X}_1, \mathrm{X}_2, \cdots, \mathrm{X}_n)$$
$$S = S(Y) = \mathrm{R}(Y_1, Y_2, \cdots, Y_n)$$

$$M = R - S = f(\mathrm{X}, \mathrm{Y}) = f(\mathrm{X}_1, \mathrm{X}_2, \cdots, \mathrm{X}_n, \mathrm{Y}_1, \mathrm{Y}_2, \cdots, \mathrm{Y}_n) \quad (14)$$

## 4. Application of Damage Mechanics in SSI

In the traditional SSI, the strength and stress of components are both static random variables. The distribution has nothing to do with time. In fact, the strength of test specimen will degrade gradually with the increase of time because of fatigue, erosion and aging. The degradation of product strength is a random process in the continual state. In this paper, the degradation of product strength consists of two parts: the first part of strength degradation is Fatigue and creep damage caused by cyclic stress, the second part is degradation of strength caused by environmental erosion and aging. In the first part, according to damage mechanics theory, in the material loading process, the fatigue cracks in part of material caused by fatigue damage and grain boundary hole in material interior created by creep damage lead to the decrease of effective loading area of section, so the effective stress increase, finally, the strength degrades.

SSI is expressed as

$$M = R - S(D_N) \quad (15)$$

On the basis of evolution Equation (11), Cumulative damage is same with the function of loading times, with the increase of loading times, the damage tends to increase. In pulsation cyclic loading, $D$ is related to initial damage, stress level and temperature, so (15) is corrected as

$$M = R - \tilde{S}(N, D_0, T, \sigma_{\max}) \quad (16)$$

The temperature $T$ not only influences damage $D$, for Q345, with the increase of temperature, strength $\sigma_s$ is yielded, ultimate strength $\sigma_b$ also showed a trend of decline. Therefore, the strength is also same with the function of temperature $T$,

$$M = R(T) - \tilde{S}(N, D_0, T, \sigma_{\max}) \quad (17)$$

Equation (17) indicates the theory of damage mechanics on the stress strength interference model.

## 5. Experiment Result Analysis

The Q345 is used as test material. Test conditions for stress control, pulsation cycle and Sine wave load are as follows. Before the test, the samples were kept in the furnace for 30 minute. The test was conducted in our libratory. The load frequency f is 0.3 Hz with stretch meter; the load frequency f is 4 Hz without stretch meter. With same temperature at 420 °C, different stress levels and the same stress level (0~480 MPa) were adopted in cycling test under different temperature (15~420 °C).

### 5.1. The Analysis of the Experimental Data under the Same Stress Level (0~480 MPa) and the Different Temperature

Seen in Table 1, the stress cycle life is the maximum at 300 °C, two curves fitting are observed in 15~420 °C.

**Table 1.** Same stress level (0~480 MPa) data with different temperatures.

| Parameter / Test specimen | $D_0$ | $k$ | $N_f$ / *cycle* | $T$ / °C |
|---|---|---|---|---|
| **1** | 0 | 0.03993 | 2571 | 15 |
| **2** | 0.0206 | 0.04994 | 3024 | 100 |
| **3** | 0.0108 | 0.07548 | 24792 | 200 |
| **4** | 0.0174 | 0.12222 | 61192 | 250 |
| **5** | 0.0198 | 0.01528 | 287366 | 300 |
| **6** | 0.0115 | 0.04036 | 84104 | 375 |
| **7** | 0.0168 | 0.03173 | 38875 | 400 |
| **8** | 0.0104 | 0.02779 | 8341 | 420 |

#### 5.1.1. The Damage Model in 15~300 °C

The relationship between $T$ and $k$ can be seen in Fig. 3.

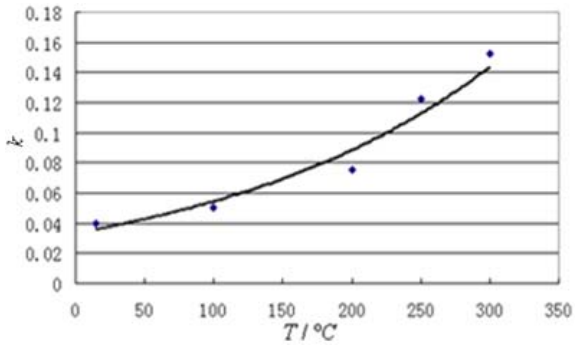


**Fig. 3.** $T$ and $k$ curve fitting at 15~420 °C.

$$k = 0.0335e^{0.0048T}$$
$$R^2 = 0.959$$

$$D = 1 - (1 - D_0)(1 - N / N_f)^{0.0335e^{0.0048T}} \quad (18)$$

### 5.1.2. The Damage Model 300~420 °C

The relationship between $T$ and $k$ can be seen in Fig. 4.

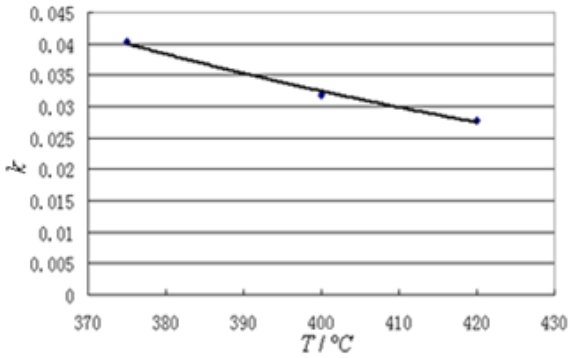


**Fig. 4.** $T$ and $k$ curve fitting at 300~420 °C.

$$k = 0.9143e^{-0.0083T}$$

$$D = 1-(1-D_0)(1-N/N_f)^{0.9143e^{-0.0083T}} \quad (19)$$

$$R^2 = 0.9897$$

### 5.2. The Test Data of the Same Temperature 420 °C under Different Stress Level

The fitting parameters of different specimens are shown in Table 2, the relationship between $k$ and $\sigma_{Max}$ can be seen in Fig. 5.

**Table 2.** Different stress levels of test data at 420 °C.

| Parameter / Test specimen | $D_0$ | $k$ | $N_f$ / *cycle* | $\sigma_{max}$ / MPa |
|---|---|---|---|---|
| **1** | 0.0134 | 0.04525 | 320614 | 0~420 |
| **2** | 0.0036 | 0.04438 | 238362 | 0~430 |
| **3** | 0.0262 | 0.04136 | 144743 | 0~440 |
| **4** | 0.0142 | 0.03963 | 91863 | 0~460 |
| **5** | 0.0307 | 0.0328 | 27302 | 0~470 |
| **6** | 0.0104 | 0.02779 | 8341 | 0~480 |
| **7** | 0 | 0.02319 | 2188 | 0~490 |

$$k = 2.2514e^{-0.0091\sigma_{max}}$$

$$R^2 = 0.8845$$

$$D = 1-(1-D_0)(1-N/N_f)^{2.2514e^{-0.0091\sigma_{max}}} \quad (20)$$

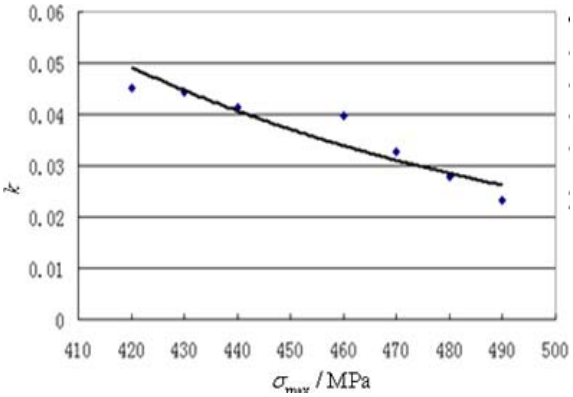


**Fig. 5.** $\sigma_{max}$ and $k$ curve fitting at 420 °C.

### 5.3. 16MnR Mechanics Performance Test Data with Different Temperatures

The mechanical properties at different temperatures are shown in Table 3, the Yield strength and ultimate strength curve fitting with different temperature can be seen in Fig. 6.

**Table 3.** Yield strength and ultimate strength test data with Different temperature.

| Temperature /°C | $\sigma_S$ / MPa | $\sigma_b$ / MPa | $\varphi$ / % |
|---|---|---|---|
| 20 | 378 | 582 | 58 |
| 100 | 312 | 516 | 63 |
| 200 | 319 | 528 | 56 |
| 300 | 283 | 576 | 52 |
| 400 | 233 | 527 | 63 |
| 420 | 238 | 517 | 70.5 |

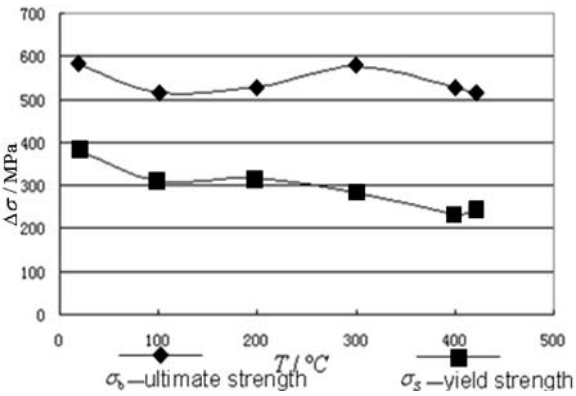


**Fig. 6.** Yield strength and ultimate strength curve fitting with different temperature.

The ultimate strength and temperature fitting function relation:

$$\begin{aligned}\sigma_b = {} & 4.072192199248056\times10^{-10}T^5 \\ & -4.412721256265577\times10^{-7}T^4 \\ & +1.544129660087676\times10^{-4}T^3 \\ & -0.017179477991850T^2 \\ & -0.178361920426170T \\ & +5.912730263157935\times10^{2}\end{aligned} \quad (21)$$

$$R^2 = 0.9671$$

## 6. Instance Analysis

The same cross section bar is shown in Fig. 7, Radius is $r = 10$ mm, under axial force $F$(kN), the material is Q345, dynamic reliability under different environmental parameters is analyzed.

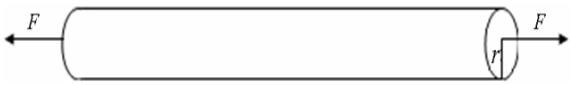


**Fig. 7.** Mechanical model of axial tension member bar.

For unidirectional tension member stress calculation is

$$S = F / A \quad (22)$$

In engineering practice, the nominal cross-sectional area $A$ of the bar is expressed as real effective area $\tilde{A}$.

Stress calculation expression:

$$S = F / \tilde{A} \quad (23)$$

By using Equation (1),

$$\tilde{A} = (1-D)A \quad (24)$$

Substituting Equation (24) into (23), we obtain,

$$S = F / A(1-D) \quad (25)$$

Then substitute (11) into (25)

$$S = F / A(1-D_0)(1-N/N_f)^{k(\sigma_{\max},T)} \quad (26)$$

By combining (17), (21) and (26),

$$M = R(T) - S(N, D_0, T, F, r) \quad (27)$$

Equation (27) demonstrates the stress strength interference function of bar.

### 6.1. Reliability Analysis with the Loading Times Sampling Test under Different Axial Tensile Force at 420 °C

1) The axial load of 135 kN, characteristic parameters are:

$\mu_F = 135\text{kN}, \sigma_F = 6.75\text{kN}$

$\mu_r = 0.01\text{m}, \sigma_r = 0.0005\text{m}$

$\mu_{D_0} = 0.0130, \sigma_{D_0} = 0.00065$

The mean and standard deviation of the ultimate strength of 420 °C are $\mu_R = 517\text{MPa}$ and $\sigma_R = 25.85\text{MPa}$, the simulation result can be seen in Fig. 8.

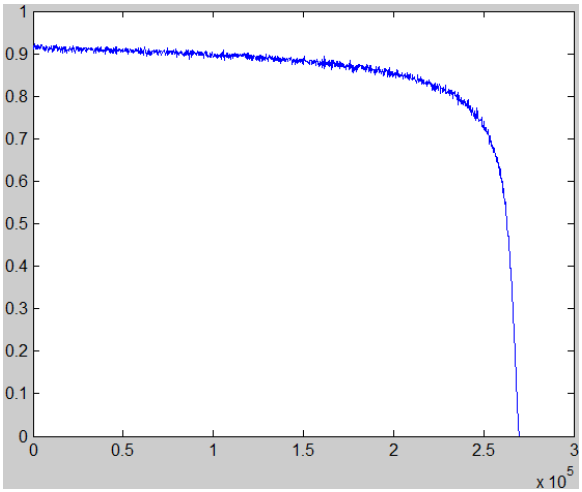


**Fig. 8.** Reliability degradation curve at 135 kN.

2) The axial load of 140 kN, characteristic parameters are:

$\mu_F = 140\text{ kN}, \sigma_F = 7\text{ kN}$

$\mu_r = 0.01\text{ m}, \sigma_r = 0.0005\text{ m}$

$\mu_{D_0} = 0.0130, \sigma_{D_0} = 0.00065$

The mean and standard deviation of the ultimate strength of 420 °C are $\mu_R = 517\text{ MPa}$ and $\sigma_R = 25.85\text{ MPa}$, the simulation result can be seen in Fig. 9.

3) The axial load of 145 kN, characteristic parameters are:

$\mu_F = 145\text{ kN}, \sigma_F = 7.25\text{ kN}$,

$\mu_r = 0.01\text{ m}, \sigma_r = 0.0005\text{ m}$

$\mu_{D_0} = 0.0130, \sigma_{D_0} = 0.00065$

The mean and standard deviation of the ultimate strength of 420 °C are $\mu_R = 517\text{ MPa}$ and $\sigma_R = 25.85\text{ MPa}$, the simulation result can be seen in Fig. 10.

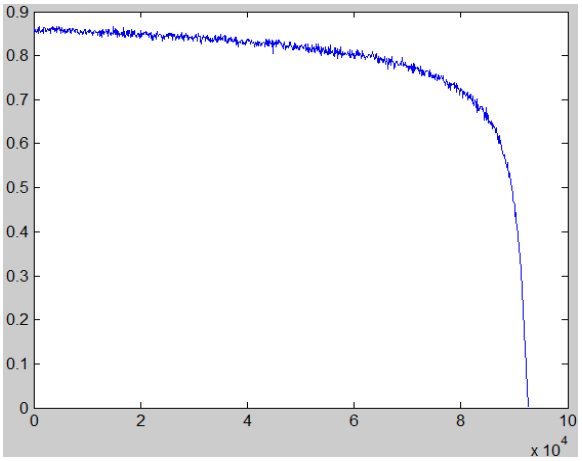


**Fig. 9.** Reliability degradation curve at 140 kN.

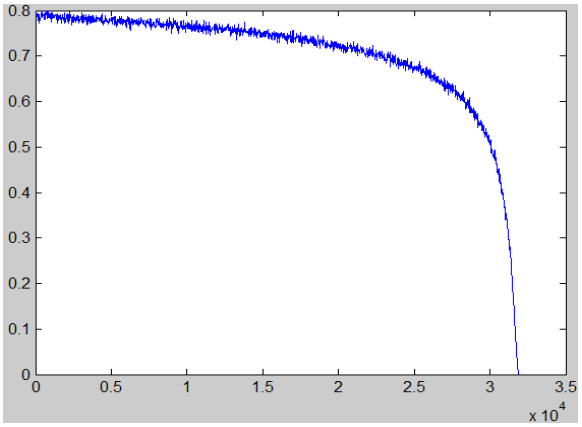


**Fig. 10.** Reliability degradation curve at 145 kN.

4) The axial load of $150\ \text{kN}$ , characteristic parameters are:

$\mu_F = 150\ \text{kN}, \sigma_F = 7.5\ \text{kN}$ ,

$\mu_r = 0.01\ \text{m}, \sigma_r = 0.0005\ \text{m}$

$\mu_{D_0} = 0.0130, \sigma_{D_0} = 0.00065$

The mean and standard deviation of the ultimate strength of 420 °C are $\mu_R = 517\ \text{MPa}$ and $\sigma_R = 25.85\ \text{MPa}$ , the simulation result can be seen in Fig. 11.

Sampling analysis experimental results of $135\ \text{kN}$ , $140\ \text{kN}$ , $145\ \text{kN}$ and $150\ \text{kN}$ showed that the greater the bar under load, the sooner an inflection point of the curve of dynamic reliability is. At the beginning of the loading cycle, the reliability declines slowly. When it is about 80 % in life, reliability decreases sharply.

Damage mechanics Damage value is indicated as $D$ using damage mechanical method. After being damaged, effective stress is obtained by using $D$ . The increasing process of effective stress is as same as that of strength degradation. Such process increases with the stretch of loading times. Assuming strength is used to explain, with the increase of loading times, the new micro crack is found in the interior of the bar. The existing micro cracks develop as the macro cracks, resulting in the decrease of the effective bearing area of the bar.

When macro crack appears, the crack tip stress concentration may improve the crack propagation speed, further weaken the carrying capacity of bar.

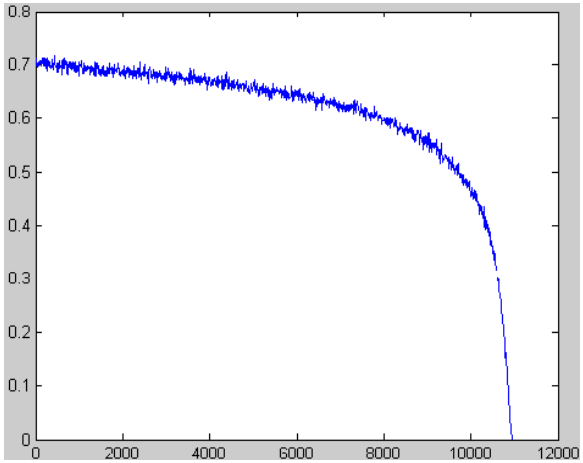


**Fig. 11.** Reliability degradation curve at 150 kN.

### 6.2. Reliability Analysis with the Loading Times Sampling Test under Same Axial Tensile Force and Different Temperatures

1) The axial load of $150\ \text{kN}$ , characteristic parameters are:

$\mu_F = 150\ \text{kN}, \sigma_F = 7.5\ \text{kN}$

$\mu_r = 0.01\ \text{m}, \sigma_r = 0.0001\ \text{m}$

$\mu_{D_0} = 0.0130, \sigma_{D_0} = 0.00065$

The mean and standard deviation of the ultimate strength of 15 °C are $\mu_R = 580\ \text{MPa}$ and $\sigma_R = 29\ \text{MPa}$ , the simulation result can be seen in Fig. 12.

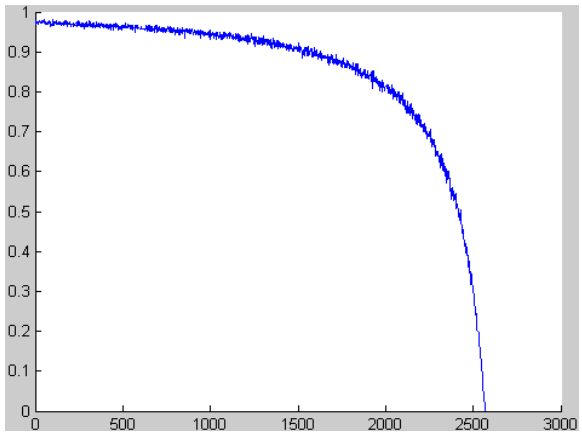


**Fig. 12.** Reliability degradation curve at 15 °C.

2) The axial load of $150\ \text{kN}$ , characteristic parameters are:

$\mu_F = 150\ \text{kN}, \sigma_F = 7.5\ \text{kN}$

$\mu_r = 0.01\ \text{m}, \sigma_r = 0.0001\ \text{m}$

$\mu_{D_0} = 0.0130, \sigma_{D_0} = 0.00065$

The mean and standard deviation of the ultimate strength of 100 ºC are $\mu_R = 516\ \text{MPa}$ and $\sigma_R = 25.8\ \text{MPa}$ ., the simulation result can be seen in Fig. 13.

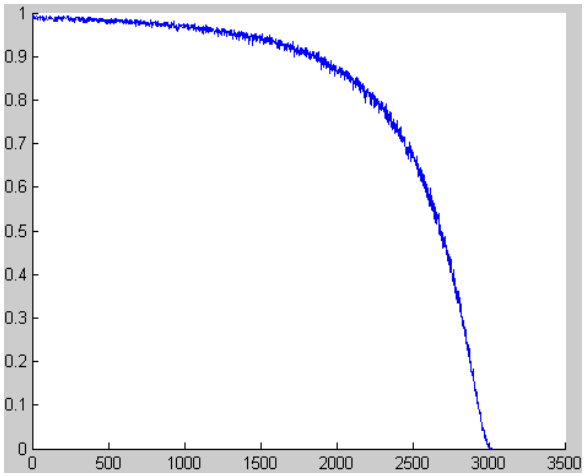


**Fig. 13.** Reliability degradation curve at 100 ºC.

3) The axial load of $150\ \text{kN}$ , characteristic parameters are:

$\mu_F = 150\ \text{kN}, \sigma_F = 7.5\ \text{kN}$

$\mu_r = 0.01\ \text{m}, \sigma_r = 0.0001\ \text{m}$

$\mu_{D_0} = 0.0130, \sigma_{D_0} = 0.00065$

The mean and standard deviation of the ultimate strength of 200 ºC are $\mu_R = 528\ \text{MPa}$ and $\sigma_R = 26.4\ \text{MPa}$ , the simulation result can be seen in Fig. 14.

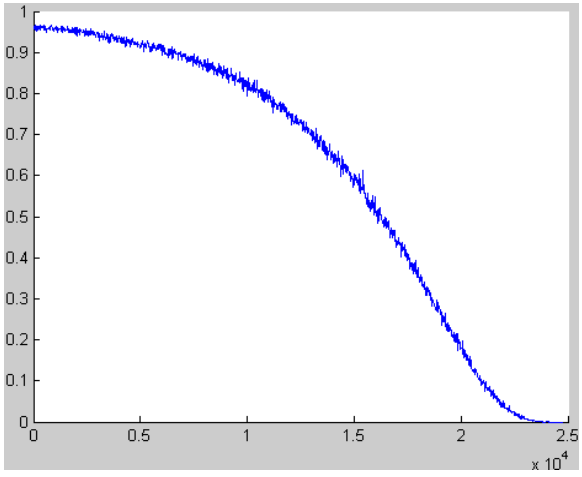


**Fig. 14.** Reliability degradation curve at 200 ºC.

4) The axial load of $150\ \text{kN}$ , the characteristic parameters are:

$\mu_F = 150\ \text{kN}, \sigma_F = 7.5\ \text{kN}$

$\mu_r = 0.01\ \text{m}, \sigma_r = 0.0001\ \text{m}$

$\mu_{D_0} = 0.0130, \sigma_{D_0} = 0.00065$

The mean and standard deviation of the ultimate strength of $300\ ^\circ C$ are $\mu_R = 576\ \text{MPa}$ and $\sigma_R = 28.8\ \text{MPa}$ , the simulation result can be seen in Fig. 15.

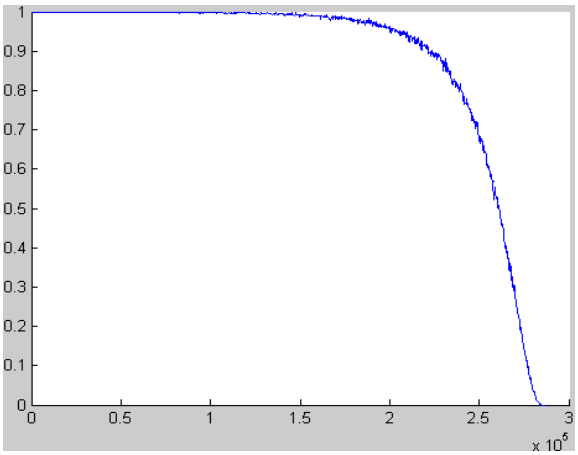


**Fig. 15.** Reliability degradation curve at 300 ºC.

5) The axial load of $150\ \text{kN}$ , the characteristic parameters are:

$\mu_F = 150\ \text{kN}, \sigma_F = 7.5\ \text{kN}$

$\mu_r = 0.01\ \text{m}, \sigma_r = 0.0001\ \text{m}$

The mean and standard deviation of the ultimate strength of 375 ºC are $\mu_R = 545\ \text{MPa}$ and $\sigma_R = 27.25\ \text{MPa}$ , the simulation result can be seen in Fig. 16.

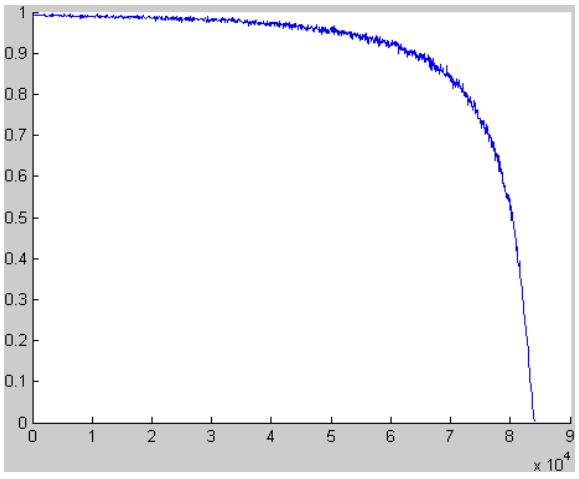


**Fig. 16.** Reliability degradation curve at 375 ºC.

6) The axial load of $150\ \text{kN}$, characteristic parameters are:

$$\mu_F = 150\ \text{kN}, \sigma_F = 7.5\ \text{kN}$$

$$\mu_r = 0.01\ \text{m}, \sigma_r = 0.0001\ \text{m}$$

$$\mu_{D_0} = 0.0130, \sigma_{D_0} = 0.00065$$

The mean and standard deviation of the ultimate strength of $400\ ^\circ C$ are $\mu_R = 527\ \text{MPa}$ and $\sigma_R = 26.35\ \text{MPa}$, the simulation result can be seen in Fig. 17.

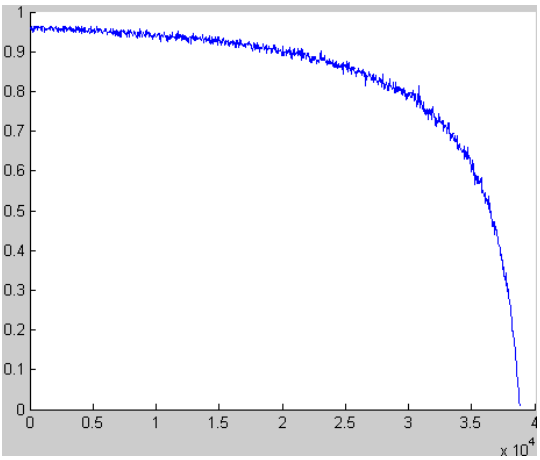


**Fig. 17.** Reliability degradation curve at 400 ºC.

7) The axial load of $150\ \text{kN}$, the characteristic parameters are:

$$\mu_F = 150\ \text{kN}, \sigma_F = 7.5\ \text{kN}$$

$$\mu_r = 0.01\ \text{m}, \sigma_r = 0.0001\ \text{m}$$

$$\mu_{D_0} = 0.0130, \sigma_{D_0} = 0.00065$$

The mean and standard deviation of the ultimate strength of $420\ ^\circ C$ are $\mu_R = 517\ \text{MPa}$ and $\sigma_R = 25.85\ \text{MPa}$, the simulation result can be seen in Fig. 18.

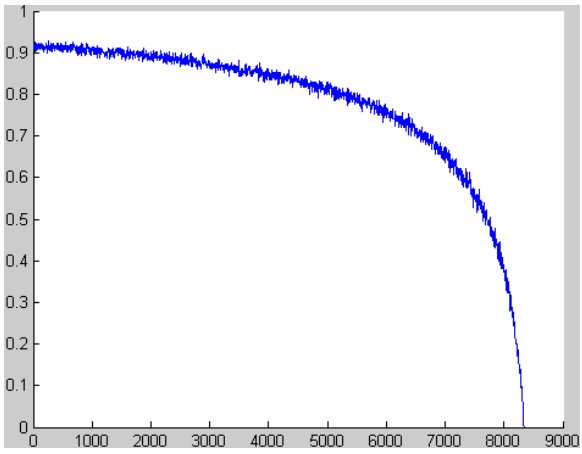


**Fig. 18.** Reliability degradation curve at 420 ºC.

Sampling test results show that when the life is about 80 %, reliability declines sharply. As the temperature rises, the closer it approaches to $300\ ^\circ C$, the later an inflection point of the curve of dynamic reliability. However, in the range from $300\ ^\circ C$ to $420\ ^\circ C$, the higher the temperature, the sooner an inflection point of the curve of dynamic reliability. This is because the 16 MNR dynamic strain aging is presented at $300\ ^\circ C$, DSA effectively curbs the development of the cyclic creep and cyclic softening phenomenon, significantly improves the cycle life, however the temperature is above $300\ ^\circ C$, larger cyclic creep and cyclic softening phenomenon result in lower material carrying capacity.

## 7. Conclusions

The dynamic reliability research of member bar of material 16MnR was made in this paper. SSI model and dynamic reliability calculation based on damage mechanics theory were put forward. The following conclusions are made by the combination of fatigue experiments with reliable sampling experiments.

1) The dynamic reliability is calculated by the combination of SSI with the damage mechanics theory, and under the direction of physical experiments. The dynamic reliability research shows the explicit physical significance.

2) In the physical experiments and sampling simulation experiments, reliable degraded curve of member bar was made with different loading and temperatures. Analyzing results indicate that reliability of member bar decreases apparently when the life is about 85 %.

3) Physical experimental data are limited, so reliable computational accuracy is expected to be improved. In the future, with the abundance of experimental data, computational accuracy will be enhanced.

## Acknowledgements

This paper is supported by the National Natural Science Foundation of China (51275329) and the National Science-technology Support Projects for the 12th five-year plan (No. 2011BAK06B05).

## References

[1]. Dilip R., Tanmoy D., A discretizing approach for evaluating reliability of complex systems under stress – strength model, *IEEE Transaction on Reliability*, 50, 2, 2001, pp. 145-150.

[2]. Sun Zhi Li, Chen Liang Yu, Zhang Yu, Ding Jin-Yuan, Reliability model of mechanical transmission system, *Journal of Northeastern University*, Dongbei Daxue Xuebao, 24, 6, 2003, pp. 548-551.

[3]. Salvatore Benfratello, Livia Cirone, Francesco Giambanco, A multicriterion design of steel frames with shakedown constraints, *Computers and Structures*, 84, 2006, pp. 269-282.
[4]. Chaudhuri A., Chakraborty S., Reliability evaluations of 3-d frame subjected to non-stationary earthquake, *Journal of Sound and Vibration*, 295, 4, 2003, pp. 797-808.
[5]. Wang Zheng, Xie Liyang, Li Bing, Time-dependent reliability model of component under random load, *Journal of Mechanical Engineering*, 43, 12, 2007, pp. 20-25.
[6]. Wang Zheng, Xie Liyang, Time-dependent reliability model and failure rate analysis of mechanical components, *Dongbei Daxue Xuebao/Journal of Northeastern University*, 28, 11, 2007, pp. 188-193.
[7]. Wang Zheng, Xie Liyang, Li Bing, Time-dependent reliability modeling and study of early failure rate for component, *Hangkong Xuebao/Acta Aeronautica et Astronautica Sinica*, 28, 6, 2007, pp. 1379-1382.
[8]. Zuo Yongzhi, Liu Xila, Fully stochastic analysis method for structural dynamic reliability, *Journal of Tsinghua University (Science and Technology)*, 44, 3, 2004, pp. 29-38.
[9]. Yu Shouwen, Feng Xiqiao, Damage mechanics, *Tsinghua University Press*, 12, Version 1, 1997, pp. 48-54.
[10]. X. H. Yang, N. Li, Z. H. Jin, T. J. Wang, A continuous low cycle fatigue damage model and its application in engineering materials, *Int. J. Fatigue*, 19, 10, 1997, pp. 687-692.
[11]. Chen Ling, Jiang Jialing, Low cycle fatigue damage model and its experimental verification, *Jinshu Xuebao/Acta Metallurgica Sinica*, 41, 2, February 2005, pp. 157-160.
[12]. D. Krajcinovic, Lemaitre J., Continuum damage mechanics, *Theory and Application*, Springer Verlag, Berlin, 1987, pp. 37-89.